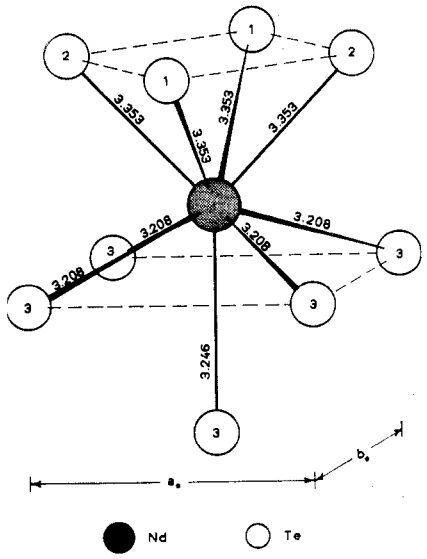

Figure 4.—Neodymium coordination polyhedron; interatomic distances are in A.

and $D(1)$ is the empirically determined single-bond distance, the sum of the single-bond radii, $R(1)$, of the two atoms involved. Pauling's values of $R(1)$ for neodymium and tellurium are 1.637 and 1.37 A, respectively.[9] The bond numbers and corresponding valences are summarized in Table IV. It should be noted that the calculated valence for the "metallic-covalent" tellurium atoms is considerably less than the formal valence for Te^{2-}.

TABLE IV
BOND DISTANCES, BOND NUMBERS, AND VALENCES

Central atom	Coordinating atom	$D(n)$	n	Σn (valence)
Nd	4 Te(3)	3.208	0.462	
	1 Te(3)	3.246	0.399	
	4 Te(1 and 2)	3.353	0.265	3.307
Te(1 and 2)	4 Te(1 or 2)	3.076	0.275	
	2 Nd	3.353	0.265	
	2 Te(3)	4.089	0.006	
	4 Te(1 and 2)	4.240	0.003	1.654
Te(3)	4 Nd	3.208	0.462	
	1 Nd	3.246	0.399	
	4 Te(3)	3.862	0.014	
	4 Te(1 and 2)	4.089	0.006	2.323

(9) L. Pauling, "The Nature of the Chemical Bond," 3rd ed, Cornell University Press, Ithaca, N. Y., 1960, p 403.

CONTRIBUTION FROM BELL TELEPHONE LABORATORIES, INCORPORATED,
MURRAY HILL, NEW JERSEY

Crystallographic Evidence for Nonequivalent Ligand Fields in Tantalum Subchloride

BY R. D. BURBANK

Received April 18, 1966

Robin and Kuebler have interpreted the electronic spectra of the polynuclear subhalides of tantalum of general formula $Ta_6X_{14}\cdot 7H_2O$ in terms of a distorted polynucleus in which two Ta at the apices of an elongated tetragonal bipyramid approach a valence of +3 while four Ta in the equator of the bipyramid approach a valence of +2. An X-ray structure analysis of $Ta_6Cl_{14}\cdot 7H_2O$ crystals is consistent with this interpretation. The crystals are trigonal, most probable space group $P\bar{3}1m$, with $a = 9.36$ A, $c = 8.80$ A, and one unit of composition per unit cell. The structure, which is both disordered and subject to faulting, contains an elongated bipyramidal polynucleus. One type of ligand field is provided for two Ta along the axis of elongation, and a second type of ligand field is provided for the remaining four Ta. The polynucleus combines with twelve Cl to form a $Ta_6Cl_{12}^{2+}$ complex ion. The complex ion combines with two Cl ions and four H_2O to form a $Ta_6Cl_{14}\cdot 4H_2O$ unit. The $Ta_6Cl_{14}\cdot 4H_2O$ units occur in layers which alternate with layers of three H_2O to yield the over-all composition of $Ta_6Cl_{14}\cdot 7H_2O$. The observed structural disorder appears to be built into the crystal during the course of crystal growth in order to permit a maximum of hydrogen bonding throughout the crystal.

Introduction

In a recent study of color and nonintegral valence Robin and Kuebler[1] have concluded that there is a fundamental difference between the niobium and tantalum subhalides. The compounds have the general formula $M_6X_{14}\cdot 7H_2O$ where M = Nb or Ta and X = Cl, Br, or I. The central building block in these compounds is the polynuclear complex ion $M_6X_{12}^{2+}$. Vaughan, Sturdivant, and Pauling[2] determined the structures of the ions $Nb_6Cl_{12}^{2+}$, $Ta_6Br_{12}^{2+}$, and $Ta_6Cl_{12}^{2+}$ in ethanol solutions using X-ray diffraction. Within the limitations imposed by the experimental technique, the scattering was satisfactorily explained by a model of cubic symmetry. The metal atoms are situated at the corners of an octahedron whose edges are ~2.9 A long. The halide atoms are on the radial perpendicular bisectors of the octahedral edges with a metal to halogen distance of ~2.4 A.

In the octahedral model of the $M_6X_{12}^{2+}$ ion, the metal atoms are all in equivalent ligand fields within the complex and the formal valence at each metal atom is $+2^1/_3$. However, if the symmetry is lower than octa-

(1) M. B. Robin and N. A. Kuebler, *Inorg. Chem.*, **4**, 978 (1965).
(2) P. A. Vaughan, J. H. Sturdivant, and L. Pauling, *J. Am. Chem. Soc.*, **72**, 5477 (1950).

hedral, the possibility arises of nonequivalent ligand fields at the metal atoms. In this case, the metal atoms will tend to trap integral valences.

Robin and Kuebler obtained the electronic spectra of the Ta and Nb subchloride and subbromide ions in aqueous and ethanol solutions at room temperature and in ethanol at $-100°$. The spectra were interpreted with a molecular orbital scheme involving both metal–metal and metal–ligand interactions. The Nb spectra could be interpreted in terms of complex ions of octahedral symmetry with nonintegral valence. Certain metal–metal bands which are degenerate in the Nb spectra were found to split in the Ta spectra, implying a lower symmetry in the subhalide ions of Ta. The symmetry was assumed to change from octahedral to an elongated tetragonal with the formal valences approaching an integral pattern of two Ta^{3+} ions at the apices of the tetragonal bipyramid and four Ta^{2+} ions in the equator of the bipyramid. In addition, the spectra of $Ta_6X_{12}^{4+}$ ions were obtained and interpreted in terms of a flattened tetragonal symmetry with two Ta^{2+} ions at the apices of the bipyramid and four Ta^{3+} ions in the equator.

It would be of considerable interest to have additional information on the symmetry of $Ta_6X_{12}^{2+}$ ions from quite different experimental methods. The present paper presents the results obtained from a structure analysis of $Ta_6Cl_{14}\cdot 7H_2O$ crystals by X-ray diffraction.

Experimental Section

The $Ta_6Cl_{14}\cdot 7H_2O$ crystals used in this investigation were selected from the specimen used by Robin and Kuebler[1] to record the spectra. The crystals were in the form of thin hexagonal plates with maximum d mensions of about 0.08×0.0025 mm. Preliminary photographic investigation was carried out on a precession camera. Because of the small size of the crystals, on the order of 10^{-8} cm^3, exposures were long and records were weak.

Systematic investigat on of a number of crystals disclosed that the symmetry was trigonal and all crystals studied were "twinned" into three components with different azimuthal orientat ons around a common orientation of the trigonal axis. The 210 point of one trigonal reciprocal lattice is coincident with the 120 point of a second lattice. The 120 point of the first lattice is also coincident with the 210 point of a third lattice. Similarly the 210 point of the second lattice is coincident with the 120 point of the third lattice. Thus only about a third of the volume of a crystal contributes to the intensity of reflections on a given reciprocal lattice. The proportions of a crystal that belonged to each of the three lattices were variable from crystal to crystal.

No space group extinctions were found and the diffraction symmetry leads to three possible space groups: $P\bar{3}1m$, P31m, or P312.

The unit cell constants were measured on precession photographs with the following results: $a = 9.36 \pm 0.03$ A, $c = 8.80 \pm 0.01$ A.

The cell was assumed to contain one unit of $Ta_6Cl_{14}\cdot 7H_2O$ leading to a calculated density of 4.25 g/cc.

Intensity measurements were made on a crystal platelet with maximum dimensions of $0.083 \times 0.083 \times 0.0025$ mm. The crystal was mounted with the trigonal axis parallel to the φ axis of a single crystal orienter. The stationary crystal technique was used with Cu Kα radiation at 40 kv, 18 ma, Ni–Co balanced filters, and 40-sec counts. The most intense reflection not affected by twinning coincidence, (010), was 42 counts/sec. Background at the larger angles was 0.5 count/sec. Reflections whose net intensity was less than three times the standard error in counting statistics were recorded as unobservable. There are 542 independent reflections permitted by the space groups within the range $2\theta < 150°$. The twinned reciprocal lattices cause coincidences for 138 of these reflections. Of the remaining reflections 125 were observable above background. The data were corrected for the Lorentz-polarization effect, overlap of the α_1,α_2 doublet, and absorption.

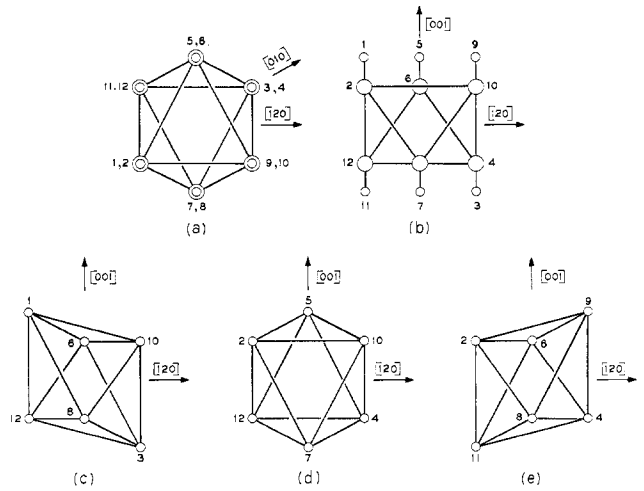

Figure 1.—(a), (b): Spatial arrangement of principal peaks in observed electron density. Large circles represent peaks of double weight. Small circles represent peaks of single weight. (c), (d), (e): Resolution of electron density into three sets of peaks defining three elongated bipyramids. Identification numbers on peaks correspond to those used in (a) and (b).

Structure Analysis

The Patterson function contained very little detail. All the resolved peaks could be accounted for by an octahedral configuration of six Ta atoms in special position $x0z$ (6k) of space group $P\bar{3}1m$ with $x = 0.181$ and $z = -0.136$, leading to a Ta–Ta distance of 2.94 A. The electron density based on the phases from this model led to the unexpected result indicated in Figure 1, (a) and (b). There were six large peaks of double weight with $x = 0.18$, $z = \cong -0.1$ which are identified in the figure by large circles with even numbers. In addition there were six peaks of single weight with $x = 0.18$, $z \cong -0.2$ which are identified in the figure by small circles with odd numbers. All these peaks were extremely elongated along the trigonal axis. The interactions of these elongated peaks had not been resolved along the c axis in the Patterson function with the result that the z parameter from the Patterson function was a weighted average of the z parameters of the peaks in the electron density. The remainder of the electron density was a profusion of small peaks, far too numerous to all be occupied by Cl or O atoms. Clearly the structure was disordered and the electron density was also subject to severe termination of series effects and lack of resolution imposed by the limited set of data that was available for the Fourier summations.

After many trials the electron density was interpreted satisfactorily in terms of the disordered model illustrated in Figure 1, (c), (d), and (e). The six Ta atoms form an elongated bipyramid which is oriented

with an inclination of about 45° to the trigonal axis. In addition the bipyramid is subject to a 3-fold disorder in azimuthal orientation around the trigonal axis. The bipyramid conforms to the monoclinic point group 2/m with the 2-fold axis passing through the origin of the unit cell perpendicular to [100], [010], or [$\bar{1}\bar{1}$0] depending on the azimuthal orientation. The apices of the bipyramid lie in the mirror plane of the monoclinic point group. The trigonal symmetry of the crystal is achieved in a statistical sense by a random distribution of the bipyramids over the three azimuthal orientations which are defined by the 3-fold axis of P$\bar{3}$1m. The eighteen peaks of the three orientations in Figure 1, (c), (d), and (e), have been given identification numbers. These peaks add up to the six double peaks and six single peaks in Figure 1, (a) and (b), with the same identification numbers.

The possibility of locating the Cl and O atoms directly from the electron density is limited by the 3-fold disorder. In an ordered structure the unit cell would contain atoms at 27 sites with unit occupancy at each site. To a first approximation the statistically averaged unit cell of the disordered structure will contain atoms at 81 sites with an occupancy factor of one-third at each site. The electron density will be characterized by poor resolution of many overlapping peaks with low peak heights.

In Table I the general positions, 12(1), of P$\bar{3}$1m have been divided into three sets of 4-fold positions which represent three monoclinic point groups which are transformed into each other by the operation of the trigonal axis. If one-third of an atom is placed in the general position of P$\bar{3}$1m this is equivalent to placing a whole atom in the general position of a monoclinic point group whose orientation is then averaged over three azimuthal settings. Similarly, if one-third of an atom is placed on a mirror plane or 2-fold axis of P$\bar{3}$1m this is equivalent to placing a whole atom on a mirror plane or 2-fold axis of a monoclinic point group. For convenience one can now think of the problem of placing whole atoms in one orientation of a monoclinic point group. Reference to Figure 2, which is based on the orientation with a 2-fold axis $\perp$ to [100], will assist in the discussion that follows.

TABLE I

DIVISION OF GENERAL POSITIONS 12(1) OF SPACE GROUP P$\bar{3}$1m INTO THREE MONOCLINIC POINT GROUPS

Orientation of 2-fold axis	General positions		Positions on mirror plane	Positions on 2-fold axis
$\perp$ to [100]	x, y, z	$x - y, \bar{y}, z$	$x, 0, z$	$x, 2x, 0$
	$y - x, y, \bar{z}$	$\bar{x}, \bar{y}, \bar{z}$	$\bar{x}, 0, \bar{z}$	$\bar{x}, 2\bar{x}, 0$
$\perp$ to [010]	$\bar{y}, x - y, z$	y, x, z	$0, x, z$	$2\bar{x}, \bar{x}, 0$
	$\bar{y}, \bar{x}, \bar{z}$	$y, y - x, \bar{z}$	$0, \bar{x}, \bar{z}$	$2x, x, 0$
$\perp$ to [$\bar{1}\bar{1}$0]	$y - x, \bar{x}, z$	$\bar{x}, y - x, z$	$\bar{x}, \bar{x}, z$	$x, \bar{x}, 0$
	$x, x - y, \bar{z}$	$x - y, x, \bar{z}$	$x, x, \bar{z}$	$x, \bar{x}, 0$

The Ta polynucleus is described by Ta(1) on the mirror plane and Ta(2) in the general position. No decisive information concerning Cl and O positions was available from the electron density. Using the Vaughan, Sturdivant, and Pauling model[2] the $Ta_6Cl_{12}^{2+}$ complex ion can be described by placing Cl(1) on the mirror plane, Cl(2) in the general position, Cl(3) on the 2-fold axis, and Cl(4) in the general position. Least-squares refinement of this model followed by a difference electron density suggested that the $Ta_6Cl_{12}^{2+}$ complex ion coordinates six additional atoms in an approximately octahedral configuration. Trial and error established that the complex ion coordinates two Cl^- ions and four H_2O molecules to form a $Ta_6Cl_{14}\cdot 4H_2O$ unit which can be described by placing Cl(5) on the mirror plane and O(1) in the general position.

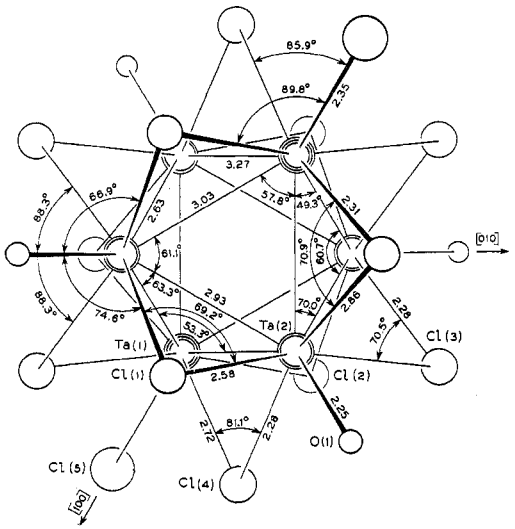

Figure 2.—Structure of the $Ta_6Cl_{14}\cdot 4H_2O$ unit.

After least-squares refinement of the $Ta_6Cl_{14}\cdot 4H_2O$ model further trial and error was used to place the remaining three H_2O molecules. The $Ta_6Cl_{14}\cdot 4H_2O$ units lie in layers normal to the trigonal axis. These layers alternate with layers composed of three H_2O per unit cell which are situated halfway between to yield the over-all composition of $Ta_6Cl_{14}\cdot 7H_2O$. The three H_2O are disordered in their layer but in a different way than the $Ta_6Cl_{14}\cdot 4H_2O$ units are disordered. The monoclinic point groups of Table I are not appropriate for describing this second type of disorder. The three H_2O are randomly distributed over the 6-fold position x, $2x$, $1/2$ (6j) of space group P$\bar{3}$1m. The six sites in 6j are occupied with an occupancy factor of one-half at each site when averaged over the entire crystal. On the average any individual unit cell will contain three sites which are occupied by whole atoms and three sites which are vacant.

The complete $Ta_6Cl_{14}\cdot 7H_2O$ diffraction model is defined by the following distribution of atoms in P$\bar{3}$1m.

$1/3$Ta(1) in $x, 0, z$
$1/3$Ta(2) in x, y, z with $y \cong x$
$1/3$Cl(1) in $x, 0, z$
$1/3$Cl(2) in x, y, z with $y \cong x$
$1/3$Cl(3) in $x, 2x, 0$
$1/3$Cl(4) in x, y, z with $y \cong 1/2x \cong x$ of Cl(3), $z \cong 0$
$1/3$Cl(5) in $x, 0, z$
$1/3$O(1) in x, y, z with $y \cong x$
$1/2$O(2) in $x, 2x, 1/2$

TABLE II

PARAMETERS FOR $Ta_6Cl_{14}\cdot 7H_2O$[a]

Atom	Position	Occupancy	x	y	z	B, A^2
Ta(1)	6k	1/3	0.1805 (0.0035)	0	−0.2030 (0.0028)	2.47 (0.44)
Ta(2)	12l	1/3	0.1808 (0.0011)	x	0.1145 (0.0009)	0.72 (0.19)
Cl(1)	6k	1/3	0.267 (0.019)	0	0.267 (0.022)	5.2 (3.4)
Cl(2)	12l	1/3	0.208 (0.007)	x	−0.364 (0.012)	3.9 (1.4)
Cl(3)	6j	1/3	0.205 (0.002)	$2x$	0	2.1 (0.7)
Cl(4)	12l	1/3	$2x$	x	0	
Cl(5)	6k	1/3	0.404 (0.015)	0	−0.325 (0.016)	2.4 (2.1)
O(1)	12l	1/3	0.344 (0.011)	x	0.303 (0.010)	−0.6 (1.8)
O(2)	6j	1/2	0.234 (0.012)	$2x$	1/2	2.7 (4.0)

[a] Least squares standard deviations in parentheses.

To appreciate the significance of the approximate equalities among certain of the parameters in the above list a notation will be used such that Ta(2) [100] and Ta(2) [010] will refer to Ta(2) atoms belonging to the $Ta_6Cl_{14}\cdot 4H_2O$ groups whose 2-fold axes of symmetry are perpendicular to [100] and [010], respectively. Referring back to Table I one can see that if $y \cong x$ then x, y, z and y, x, z will be defining almost the same position in space, similarly for the remaining general positions taken in pairs. This means that Ta(2) [100] at x, y, z overlaps Ta(2) [010] at y, x, z, Ta(2) [100] at $y - x, y, \bar{z}$ overlaps Ta(2) [$\bar{1}\bar{1}0$] at $x - y, x, \bar{z}$, and so on. The diffraction model was refined by least squares with the variables listed above until the separation between pairs of Ta(2) atoms had decreased to 0.008 A. This quantity was less than half of the standard error associated with defining the position of a Ta(2) atom. Accordingly y of Ta(2) was eliminated as a variable and set equal to x of Ta(2) in the remaining refinement. The same considerations were applied when the separation between pairs of O(1) atoms had decreased to 0.067 A and when the separation between pairs of Cl(2) atoms had decreased to 0.070 A. Referring the relations among the parameters of Cl(4) and Cl(3) back to Table I one can see that Cl(4) [100] at x, y, z and Cl(4) [$\bar{1}\bar{1}0$] at $x, x - y, \bar{z}$ will overlap Cl(3) [010] at $2x, x, 0$, Cl(4) [100] at $y - x, y, \bar{z}$, and Cl(4) [010] at $\bar{y}, x - y, z$ will overlap Cl(3) [$\bar{1}\bar{1}0$] at $\bar{x}, x, 0$, and so on. The least-squares refinement was continued until the separation between pairs of Cl(4) atoms had decreased to 0.078 A and the separation between Cl(4) and Cl(3) atoms had decreased to 0.054 A. At this point z of Cl(4) was fixed at 0, y of Cl(4) was eliminated as a variable and set equal to x of Cl(3), and x of Cl(4) was eliminated as a variable and set equal to $2x$ of Cl(3).

Least-squares refinement of the final model involved 14 positional parameters and 8 isotropic thermal parameters. Form factors for Cl and O^- were taken from Table 3.3.1A and for Ta from Table 3.3.1B of the International Tables.[3] The function minimized was $\Sigma w(F_o - F_c)^2$ with $w = 1$ for the 125 observed structure factors. At the end of the refinement the R factor was 0.127, where $R = \Sigma|F_o - F_c|/\Sigma|F_o|$, and wR was 0.143, where $wR = \sqrt{\Sigma w(F_o - F_c)^2}/\sqrt{\Sigma w F_o^2}$. The final list of parameters is presented in Table II. The negative value of the thermal parameter B for O(1) is only one-third of the standard deviation and has no physical significance. A comparison of the observed and calculated structure factors is presented in Table III.

TABLE III

COMPARISON OF F_o AND F_c

hkℓ	$\|F_o\|$	$\|F_c\|$	hkℓ	$\|F_o\|$	$\|F_c\|$	hkℓ	$\|F_o\|$	$\|F_c\|$	hkℓ	$\|F_o\|$	$\|F_c\|$
000	-	607	1·3·10	20	23	341	134	133	$\bar{1}$82	66	63
010	230	256	150	143	154	342	143	128	$\bar{1}$91	106	115
011	89	118	151	78	68	344	82	80	$\bar{1}$92	76	85
012	50	60	153	91	91	345	69	69	$\bar{1}$95	48	48
013	53	111	154	91	102	348	31	28	$\bar{2}$41	194	193
014	66	119	160	54	70	372	54	62	$\bar{2}$42	186	183
020	111	82	161	69	68	373	57	46	$\bar{2}$44	116	131
021	63	47	172	96	104	441	172	162	$\bar{2}$45	100	97
030	117	98	182	91	82	442	125	123	$\bar{2}$48	38	44
031	108	93	183	62	71	444	78	47	$\bar{2}$49	37	45
032	62	53	220	184	158	445	61	63	$\bar{3}$51	145	151
033	66	58	222	296	304	447	36	49	$\bar{3}$52	87	83
040	110	109	223	166	167	448	32	30	$\bar{3}$76	46	34
050	345	310	225	45	28	456	43	26	$\bar{3}$84	58	53
051	193	152	226	38	36	550	106	128	$\bar{3}$91	108	123
054	81	93	227	53	82				$\bar{3}$92	108	105
060	208	199	229	29	47	$\bar{1}$21	82	84	$\bar{3}$94	71	58
061	132	105	2·2·10	24	31	$\bar{1}$22	71	86	$\bar{3}$95	69	64
063	127	104	230	100	93	$\bar{1}$23	41	81	$\bar{4}$62	150	134
064	98	116	232	77	61	$\bar{1}$25	37	29	$\bar{4}$63	111	100
065	72	77	233	58	52	$\bar{1}$26	32	34	$\bar{4}$69	28	33
066	56	38	253	63	36	$\bar{1}$41	178	176	$\bar{4}$72	177	171
0·10·0	66	91	262	113	89	$\bar{1}$42	123	138	$\bar{4}$73	123	118
0·10·1	57	56	270	74	76	$\bar{1}$41	47	25	$\bar{4}$76	55	39
111	100	109	272	120	136	$\bar{1}$45	52	48	$\bar{5}$·10·1	81	91
112	92	112	273	89	101	$\bar{1}$49	28	26	$\bar{5}$·10·5	36	29
115	27	30	276	41	34	$\bar{1}$61	117	108	$\bar{5}$·11·1	38	18
130	117	97	331	65	59	$\bar{1}$63	96	94	$\bar{5}$·8·2	146	131
131	85	77	332	60	53	$\bar{1}$64	90	95	$\bar{5}$·8·3	97	90
132	125	123	334	94	101	$\bar{1}$65	52	51	$\bar{5}$·8·6	51	46
133	70	67	335	50	39	$\bar{1}$66	47	39	$\bar{5}$·10·5	35	21
136	46	62	340	68	61	$\bar{1}$73	63	65			

The various calculations were carried out on an IBM 7094 computer using the Sly, Shoemaker, and Van den Hende Fourier program,[4] the Busing, Martin, and Levy least-squares program,[5] and the Busing, Martin, and Levy function and error program.[6]

Structure of the $Ta_6Cl_{14}\cdot 4H_2O$ Unit

The $Ta_6Cl_{14}\cdot 4H_2O$ unit is illustrated in Figure 2 for the [100] azimuthal orientation. The bond distances and bond angles are summarized in the figure and in Table IV. The Ta_6 polynucleus forms an elongated bipyramid. Twelve Cl atoms are situated approximately on the radial perpendicular bisectors of the bipyramidal edges to form the $Ta_6Cl_{12}^{2+}$ complex ion. The twelve Cl atoms form a polyhedron enclosing the polynucleus which has eight triangular faces and six approximately rectangular faces. The complex ion forms the $Ta_6Cl_{14}\cdot 4H_2O$ unit by coordinating two Cl^- ions and four H_2O molecules at the approximate centers of the six rectangular faces. The two Cl^- ions and

(3) "International Tables for X-Ray Crystallography," Vol. III, Kynoch Press, Birmingham, 1962.

(4) W. G. Sly, D. P. Showmaker, and J. H. Van den Hende, Esso Research and Engineering Co. Report CBRL-22M-62 (1963).

(5) W. R. Busing, K. O. Martin, and H. A. Levy, Oak Ridge National Laboratory Report TM-305 (1962), modified by B. B. Cetlin.

(6) W. R. Busing, K. O. Martin, and H. A. Levy, Oak Ridge National Laboratory Report TM-306 (1964).

TABLE IV

BOND DISTANCES AND ANGLES IN THE $Ta_6Cl_{14}\cdot 4H_2O$ UNIT[a,b]

Distances, A		Angles, deg	
Ta(1)–Ta(2)	3.27 (0.03)	Ta(2)–Ta(1)–Ta(2″)	53.3 (0.6)
Ta(1)–Ta(2′)	3.03 (0.03)	Ta(2′)–Ta(1)–Ta(2‴)	57.8 (0.7)
Ta(2)–Ta(2′)	2.63 (0.01)	Ta(2)–Ta(1)–Ta(2′)	49.2 (0.4)
		Ta(2′)–Ta(2)–Ta(1)	60.7 (0.6)
		Ta(2′)–Ta(2)–Ta(1′)	70.0 (0.5)
Ta(2)–Ta(2″)	2.93 (0.02)	Ta(2″)–Ta(2)–Ta(1)	63.3 (0.3)
		Ta(2″)–Ta(2)–Ta(1′)	61.1 (0.4)
Cl(1)–Ta(2)	2.58 (0.15)	Ta(2)–Cl(1)–Ta(2″)	69.2 (4.6)
Cl(2)–Ta(1)	2.31 (0.08)		
Cl(2)–Ta(2′)	2.86 (0.09)	Ta(1)–Cl(2)–Ta(2′)	70.9 (2.8)
Cl(3)–Ta(2)	2.28 (0.03)	Ta(2)–Cl(3)–Ta(2′)	70.5 (1.0)
Cl(4)–Ta(1)	2.72 (0.03)		
Cl(4)–Ta(2)	2.28 (0.03)	Ta(1)–Cl(4)–Ta(2)	81.1 (1.2)
Cl(5)–Ta(1)	2.35 (0.14)	Cl(5)–Ta(1)–Cl(2)	89.8 (3.1)
		Cl(5)–Ta(1)–Cl(4)	84.9 (2.7)
O(1)–Ta(2)	2.25 (0.10)	O(1)–Ta(2)–Cl(1)	74.6 (3.0)
		O(1)–Ta(2)–Cl(2′)	66.9 (2.5)
		O(1)–Ta(2)–Cl(3)	88.3 (1.8)
		O(1)–Ta(2)–Cl(4)	88.3 (1.8)

[a] Least-squares standard deviations in parentheses. [b] Single, double, and triple primes refer to atoms related to reference atom by rotation, reflection, and inversion, respectively.

four H_2O molecules form an elongated bipyramid "enclosing" the complex ion.

The nonbonded nearest neighbors in the $Ta_6Cl_{14}\cdot 4H_2O$ unit are summarized in Table V. From Figure 2 and Tables IV and V the environment for each type of atom may be described. The Ta(1) atom is bonded to nine neighbors including four Ta(2) and four Cl atoms in the complex ion plus one Cl^- ion. The Ta(2) atom is bonded to nine neighbors including two Ta(1), two Ta(2), and four Cl atoms in the complex ion plus one H_2O molecule. The Cl(1) and Cl(3) atoms are each bonded to two Ta(2) and have six other neighbors including four Cl atoms in the complex ion and two H_2O molecules. The Cl(2) and Cl(4) atoms are each bonded to one Ta(1) and one Ta(2) and have six other neighbors including four Cl atoms in the complex ion, one Cl^- ion, and one H_2O molecule. The Cl(5) atom is bonded to one Ta(1) and has four Cl neighbors in the complex ion. The O(1) atom is bonded to one Ta(2) and has four Cl neighbors in the complex ion.

Various geometrical quantities relating to the bipyramids formed by the Ta_6 polynucleus and by the $2Cl^- + 4H_2O$ coordination group are summarized in Table VI. Of central chemical significance is the very large difference of 0.98 (0.07) A between the Ta(1)–Ta(1′) and Ta(2)–Ta(2‴) distances. This is a direct measure of the elongation of the polynucleus and supports the interpretation that the Ta(1) atoms approach a +3 valence and the Ta(2) atoms approach a +2 valence. The bipyramid of two Cl^- ions and four H_2O molecules is elongated to about the same extent as the polynucleus as indicated by the difference of 1.12 (0.29) A between Cl(5)–Cl(5′) and O(1)–O(1‴). Although Cl(5) lies 19.3° (3.6°) off the Ta(1)–Ta(1′) axis and O(1) lies 16.5° (2.5°) off the Ta(2)–Ta(2‴) axis there is no question that the Cl^- ions are coordinated by the most positive regions of the polynucleus at Ta(1) and Ta(1′).

TABLE V

ENVIRONMENT OF NONBONDED NEAREST NEIGHBORS IN THE $Ta_6Cl_{14}\cdot 4H_2O$ UNIT (A)[a]

Cl(1)–2Cl(2)	3.95 (0.17)	Cl(2)–Cl(1)	3.95 (0.17)
Cl(1)–2Cl(4)	2.91 (0.16)	Cl(2)–Cl(2)	3.36 (0.12)
Cl(1)–2O(1)	2.94 (0.09)	Cl(2)–Cl(3)	3.73 (0.09)
		Cl(2)–Cl(4)	3.73 (0.09)
		Cl(2)–Cl(5)	3.29 (0.12)
		Cl(2)–O(1)	2.86 (0.08)
Cl(3)–2Cl(2)	3.73 (0.09)	Cl(4)–Cl(1)	2.91 (0.16)
Cl(3)–2Cl(4)	3.33 (0.03)	Cl(4)–Cl(2)	3.73 (0.09)
Cl(3)–2O(1)	3.16 (0.08)	Cl(4)–Cl(3)	3.33 (0.03)
		Cl(4)–Cl(4)	3.33 (0.03)
		Cl(4)–Cl(5)	3.43 (0.12)
		Cl(4)–O(1)	3.16 (0.08)
Cl(5)–2Cl(2)	3.29 (0.12)	O(1)–Cl(1)	2.94 (0.09)
Cl(5)–2Cl(4)	3.43 (0.12)	O(1)–Cl(2)	2.86 (0.08)
		O(1)–Cl(3)	3.16 (0.08)
		O(1)–Cl(4)	3.16 (0.08)

[a] Least-squares standard deviations in parentheses.

TABLE VI

GEOMETRICAL DISTANCES AND ANGLES IN THE BIPYRAMIDAL Ta_6 POLYNUCLEUS AND IN THE BIPYRAMIDALLY COORDINATED $2Cl^- + 4H_2O$ GROUP[a]

Ta(1)–Ta(1′), A	4.92 (0.06)	Difference
Ta(2)–Ta(2‴), A	3.94 (0.02)	0.98 (0.07)
Ta(1)–origin–Ta(2), deg	94.4 (0.5)	
Ta(2)–origin–Ta(2″), deg	96.2 (0.3)	
Cl(5)–Cl(5′), A	9.48 (0.28)	Difference
O(1)–O(1‴), A	8.36 (0.20)	1.12 (0.29)
Cl(1)–origin–O(1), deg	94.4 (1.4)	
O(1)–origin–O(1″), deg	83.8 (2.0)	
Cl(5)–Ta(1)–Ta(1′), deg	160.7 (3.6)	
O(1)–Ta(2)–Ta(2′), deg	163.5 (2.5)	

[a] Least-squares standard deviations in parentheses.

Structure of the $Ta_6Cl_{14}\cdot 7H_2O$ Crystal

The $Ta_6Cl_{14}\cdot 4H_2O$ units are arranged in layers normal to the trigonal axis. A given unit has eight closest neighboring units, six in the same layer, and two more directly above and below in the adjoining layers. However, there are very few close contacts between these units which could be expected to exert any restriction on the azimuthal orientation assumed by any given unit.

The shortest distance between two units lying one above the other in adjacent layers is 3.09 (0.17) A between two Cl(2) atoms. If the two units have the same azimuthal orientation there are two of these contacts. If the two units have different orientations there are four of these contacts. When a unit is considered with its two neighbors, above and below, there are four possibilities for Cl(2)–Cl(2) contacts: 2 + 2, 4 + 2, 2 + 4, or 4 + 4. All other distances between units in adjacent layers are 3.96 (0.21) A or greater.

The shortest distance between two adjacent units in the same layer is 3.13 (0.23) A between Cl(1) and Cl(5) atoms. This contact will occur if the azimuthal orientation of the units coincides with the direction of

the translation between the units, *i.e.*, if they are lined up "head to tail," in which case there will be a pair of contacts. Since there are six units adjacent to a given unit in a layer and each of the seven units may have one of three orientations there are many possible environments for the central unit. However, there are only two possibilities at the "head" of the unit and two at the "tail" so that there are four possibilities for Cl(1)–Cl(5) contacts: 0 + 0, 2 + 0, 0 + 2, or 2 + 2. All other distances between units in the same layer are 3.66 (0.14) A or greater.

The three H_2O molecules represented by the statistical distribution of O(2) over the sites of position 6j are the source of the forces which hold the $Ta_6Cl_{14}\cdot 4H_2O$ units together in an extended three-dimensional array of macroscopic trigonal symmetry. The nature of the sites in 6j is dependent on the azimuthal orientations of the $Ta_6Cl_{14}\cdot 4H_2O$ units as illustrated in Figure 3. In Figure 3 (a) the bottom surface of a unit with [100] orientation and the top surface of the next unit below with the same [100] orientation are shown. In Figure 3 (b) the upper unit has [100] orientation and the lower unit has $[\bar{1}\bar{1}0]$ orientation. Each site in 6j makes two contacts to the upper unit and two contacts to the lower unit. There are four types of possible contact: to Cl(1) at 2.91 (0.17) A, to Cl(2) at 2.62 (0.17) A, to Cl(5) at 2.49 (0.11) A, to O(1) at 2.58 (0.09) A. The differences in the distances to Cl(1), Cl(2), and Cl (5) are all less than the standard deviation in the associated errors, and the distances may be assumed to be equivalent. The sites then fall into three classes which are designated in Figure 3 by X, Y, and Z: X, two O(1) contacts and two Cl contacts; Y, one O(1) contact and three Cl contacts; Z, four Cl contacts. As indicated in Figure 3 when the orientation of the two units is the same there are two X sites, when the orientation of the two units is different there are three X sites. This effect suggests an interpretation of the disorder which, although it is speculative, is quite reasonable.

As indicated in Figure 3, pairs of sites in position 6j subtend an angle of 95.1° (4.2°) at O(1), and an angle of 133.7° (8.9°) is subtended at the X sites by two O(1) in neighboring units of adjacent layers. It is presumed that the crystal is held together by hydrogen bonds between H_2O molecules represented by O(1) and O(2). There will be no net bonding between neighboring $Ta_6Cl_{14}\cdot 4H_2O$ units in adjoining layers *via* an O(2) atom unless the atom is on an X site. If the two units have different orientations there will be three X sites between them instead of two, representing a 50% increase in bonding. Therefore the crystal energy will be lowered if the orientation of the units is continually changing as we proceed along a vertical stack. The change in orientation can be either + or −120° at every step. Since no definite sequence is required, the result is a disordered structure rather than a super structure.

Within a given layer of $Ta_6Cl_{14}\cdot 4H_2O$ units the bonding proceeds through pairs of O(2) atoms *via* the sequence O(1)–O(2)–O(2)–O(1) as indicated in Figures 4 and 5. Bonded pairs of O(2) atoms occur at a separation O(2)–O(2) = 2.78 (0.34) A in layers above or below the layer of $Ta_6Cl_{14}\cdot 4H_2O$ units. At one end of an O(2)–O(2) bond an O(1) atom subtends an angle O(1)–O(2)–O(2) = 91.6° (4.2°), while at the other end of the bond an O(1) atom subtends an angle O(2)–

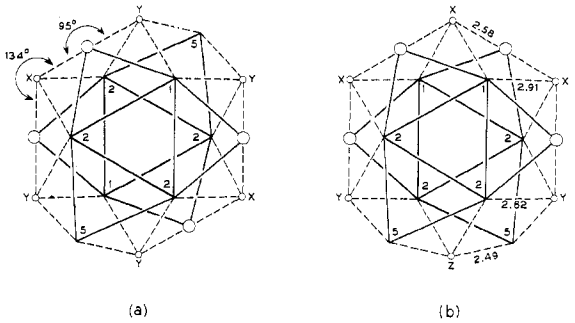

Figure 3.—Possible sites for O(2) atoms between $Ta_6Cl_{14}\cdot 4H_2O$ units in adjoining layers. Vertices numbered 1, 2, and 5 correspond to Cl (1), Cl (2), and Cl (5) atoms in the bottom surface of one unit and in the top surface of the next unit below. Large circles represent O(1) atoms, small circles represent potential O(2) sites.

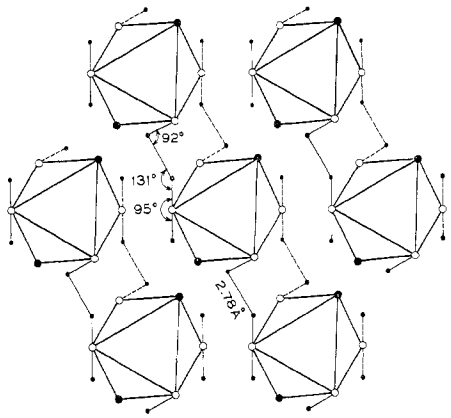

Figure 4.—Bonding within a layer of $Ta_6Cl_{14}\cdot 4H_2O$ units with a common [100] azimuthal orientation. Bipyramids of $2Cl^- + 4H_2O$ are represented by large solid dots for Cl(5), open circles for O(1). Small dots represent O(2). Solid lines between O(2) indicate hydrogen bonds at $z = +1/2$, dotted lines between O(2) indicate hydrogen bonds at $z = -1/2$.

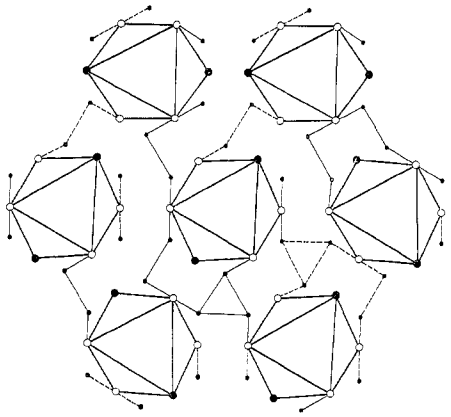

Figure 5.—Bonding within a layer of $Ta_6Cl_{14}\cdot 4H_2O$ units with a random distribution of azimuthal orientation. Symbols as for Figure 4.

O(2)–O(1) = 130.8 (3.9°). In Figure 4 all the $Ta_6Cl_{14}\cdot 4H_2O$ units are depicted with a common [100] azimuthal orientation. The O(2)–O(2) bonds form a regular pattern such that each unit is bonded to two of its six neighboring units through four O(2)–O(2) bonds. In Figure 5 the units are depicted with a random distribution of azimuthal orientation. The central unit is bonded to five of its six neighboring units through seven O(2)–O(2) bonds. Again the crystal energy will be lowered if the orientation of the units is quite haphazard throughout a layer.

To summarize the preceding discussion, it is proposed that the observed disorder is built into the crystal during the course of crystal growth in order to permit a maximum of hydrogen bonding throughout the crystal.

To complete the description of the structure, it remains to interpret the "twinning" phenomena observed on the diffraction patterns. Translated into real space there is a second lattice whose orientation relative to the first lattice is defined by reflection of the first lattice across its (210) plane. There is a third lattice whose orientation relative to the first lattice is defined by reflection of the first lattice across its (120) plane. If the structure is thought of in terms of layers, then the possibility arises than an occasional stacking fault may occur in the process of crystal growth. Figure 6 illustrates one of the two types of faulted orientation from layer to layer that would explain the diffraction patterns. The variability to be expected in any faulting process would be consistent with the observed variation from crystal to crystal in the relative magnitudes of the three diffraction components. A stacking fault would create a disruption in the regularity of the layer to layer spacing which might be expected to create diffuse streaks in the diffraction in a direction normal to the layers. In fact, the (010) reflection, which is the strongest reflection not superimposed on "twinned" reflections, was observed to have this type of diffuse streak. No other diffuse scattering was observed, presumably because of the extremely weak diffraction records.

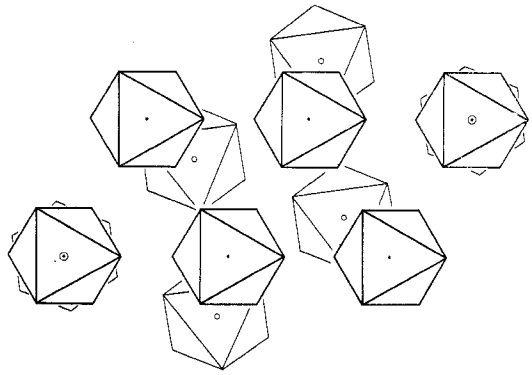

Figure 6.—Type of stacking fault which would give rise to observed twinning of crystals. Octahedra represent bipyramids of $2Cl^- + 4H_2O$. Octahedra centered on solid dots represent a layer of structure of the "parent" lattice. Octahedra centered on open circles represent a layer with faulted orientation. The faulted orientation is related to the unfaulted orientation by reflection across (210) of the "parent" lattice. A second faulted orientation, not illustrated, is defined by reflection across (120).

Discussion

New information on the structures of anhydrous tantalum and niobium subhalides has been reported very recently by Schäfer and co-workers.[7-9] Nb_6Cl_{14}[7] and Ta_6I_{14}[8] are isostructural in the sense that both compounds crystallize in the same orthorhombic space group, with complete correspondence in the location of atoms in various symmetry positions. The $M_6X_{12}^{2+}$ ions share four X^- ions equally with four neighboring complex ions to form extended sheets of composition M_6X_{14}. In both cases the M_6 polynuclei form a flattened octahedron instead of an elongated octahedron. This is interpreted by Schäfer, *et al.*, in terms of four metal atoms in the base with a valence of +2.5 and two atoms at the apices with a valence of +2. There appears to be a significant difference in the relative distortion of the metal polynucleus in the two compounds. The flattened distortion is much more pronounced for Ta than for Nb. In Nb_6Cl_{14} the average difference between the long and short Nb–Nb bonds is 0.06 A. In Ta_6I_{14} the average difference between the long and short Ta–Ta bonds is 0.275 A.

The compound Nb_6F_{15} is cubic.[9] The $Nb_5F_{12}^{3+}$ ions share six F^- ions equally with six neighboring complex ions to form an extended three-dimensional network of composition Nb_6F_{15}. The Nb_6 polynucleus has full octahedral symmetry and all six metal atoms have a valence of +2.5.

There appears to be a structural principle which is common to all these polynuclear subhalides, both hydrated and anhydrous. In every case, there is a complex ion of the form $M_6X_{12}^{n+}$. The polyhedron formed by the twelve halide ions around the polynucleus has six square faces (assuming no distortion) and eight triangular faces. Additional ligands are invariably coordinated at the centers of some or all of the six square faces. The ligands either form a complete octahedral configuration around the complex ion or occupy a portion of the octahedral sites. In the M_6X_{14} compounds four of these sites are occupied by X^- and two are unoccupied. In the M_6X_{15} compounds all six sites are occupied by X^-. In the $M_6X_{14}\cdot nH_2O$ compounds two sites are occupied by X^- and four sites are occupied by H_2O.

In the crystalline state two points are clear. First, the $M_6X_{12}^{n+}$ ion coordinates additional ligands in an octahedral pattern. Second, the Ta polynucleus is subject to large deformations while the Nb polynucleus is not. It seems reasonable that the sense of the deformations, *i.e.*, flattening or elongation, is dictated by the crystal forces. A consistent pattern is followed with four negative ligands leading to a flattening, two negative ligands leading to an elongation, and six nega-

(7) A. Simon, H. G. Schnering, H. Wöhrle, and H. Schäfer, *Z. Anorg. Allgem. Chem.*, **339**, 155 (1965).

(8) D. Bauer, H. G. Schnering, and H. Schäfer, *J. Less-Common Metals*, **8**, 388 (1965).

(9) H. Schäfer, H. G. Schnering, K. J. Niehues, and H. G. Nieder-Vahrenholz, *ibid.*, **9**, 95 (1965).

tive ligands leaving the equilibrium symmetry undisturbed.

The evidence concerning the $M_6X_{12}^{n+}$ ions in solutions is more complicated.[1] Again it is clear that the Ta polynucleus is subject to large deformations while the Nb polynucleus is not. The sense of the deformations is such that it would be consistent with hexasolvated complex ions with two X^- and four H_2O solvated to the elongated $Ta_6X_{12}^{2+}$ ions and four X^- and two H_2O solvated to the flattened $Ta_6X_{12}^{4+}$ ions. However, the spectroscopic evidence does not support this view. Robin[10] and Kuebler found an identical splitting of the metal–metal bands for the $Ta_6Cl_{12}^{2+}$ ion when the anionic species was any one of Cl^-, OH^-, ClO_4^-, or CN^-. If these various anions were solvating the $Ta_6Cl_{12}^{2+}$ ion, the spectral splitting would be expected to be different in each case.

Acknowledgment.—The author wishes to thank M. B. Robin for suggesting this problem, for providing the $Ta_6Cl_{14}\cdot 7H_2O$ crystals, and for helpful and stimulating discussion.

(10) M. B. Robin, private communication.

CONTRIBUTION FROM THE WILLIAM RAMSAY AND RALPH FORSTER LABORATORIES, UNIVERSITY COLLEGE, LONDON, ENGLAND

The Crystal Structure of Bis(triphenylmethylarsonium)tetrachloronickel(II), $[(C_6H_5)_3CH_3As]_2[NiCl_4]$, of the Isomorphous Compounds of Mn, Fe, Co, and Zn, and of the Corresponding Bromides

BY PETER PAULING

Received July 20, 1965

The crystal structure of bis(triphenylmethylarsonium)tetrachloronickel(II), $[(C_6H_5)_3CH_3As]_2[NiCl_4]$, has been determined from the three-dimensional sharpened Patterson function and phased observed Fourier syntheses and refined by least-squares methods. Crystals of the compound are cubic, space group T_4-$P2_13$, $a_0 = 15.557 \pm 0.004$ A with four formula units per unit cell. The crystals contain the tetrachloronickel ion, $[NiCl_4]^{2-}$, and two crystallographically distinct kinds of the triphenylmethylarsonium ion, $[(C_6H_5)_3CH_3As]^+$. The arsenic and nickel atoms, one of the four chlorine atoms, and the carbon atoms of the methyl groups lie in special positions of the space group on threefold axes. All the complex ions are tetrahedral, the three phenyl groups of each arsonium ion being crystallographically equivalent and three of the chlorine atoms of each tetrachloronickel ion being crystallographically equivalent. The $[NiCl_4]^{2-}$ group is regularly tetrahedral to within experimental error, the Ni–Cl distances being 2.267 ± 0.008 and 2.271 ± 0.007 A and the Cl–Ni–Cl angles being $109° 19' \pm 14'$ and $109° 38' \pm 17'$. Crystals of the corresponding compounds containing the complex ions $[MnCl_4]^{2-}$, $[FeCl_4]^{2-}$, $[CoCl_4]^{2-}$, $[ZnCl_4]^{2-}$, $[MnBr_4]^{2-}$, $[CoBr]^{2-}$, $[NiBr_4]^{2-}$, and $[ZnBr_4]^{2-}$ have been shown by single-crystal and powder diffraction photographs to be isomorphous with the compound containing the $[NiCl_4]^{2-}$ ion. Crystals of the corresponding compounds of $[CuCl_4]^{2-}$ and $[CuBr_4]^{2-}$ are isomorphous with each other; those of the chloride are orthorhombic, $a = 32.27 \pm 0.02$, $b = 25.24 \pm 0.02$, $c = 8.943 \pm 0.003$ A, space group Fdd2, eight formula units per unit cell. Crystals of the tetraiodides of Mn, Fe, Co, Ni, and Zn are isomorphous with each other but have a different crystal structure from the chlorides and bromides.

Introduction

Of the several high-symmetry ligancy forms adopted by transition metal coordination compounds, the regularly tetrahedral form has been extensively discussed in recent years. One of the major problems is why it does not occur more often in certain electronic configurations such as d^2 or d^8. According to simple chemical bond[1] theory, paramagnetic tetrahedral nickel(II) should be stable. Most of the compounds thought to contain tetrahedral nickel(II), such as bis(acetylacetonato)nickel(II), have turned out to be polymeric and have octahedral coordination.[2]

An explanation for the difficulty[3] in finding tetrahedrally coordinated nickel(II) compounds has been put forward by Orgel[4] by a consideration of the interaction of the electrostatic field of the ligands and the d electrons of the metal. For this effect alone the tetrahedral configuration is destabilized relative to the octahedral configuration because of the splitting of the d electron shells by the cubic fields. Furthermore, according to the theory of Jahn and Teller,[5] wherever there might exist degeneracy in the electronic states with a symmetric structure, there exists a more stable nondegenerate state with a less symmetric structure. Therefore, since regularly tetrahedrally coordinated nickel(II) is degenerate in d_ϵ electronic states we expect the configuration to distort in some manner as to remove this degeneracy.

(1) L. Pauling, *J. Am. Chem. Soc.*, **53**, 1367 (1931); L. Pauling, "The Nature of the Chemical Bond," 3rd ed, Cornell University Press, Ithaca, N. Y., 1960, pp 153, 168.

(2) G. J. Bullen, R. Mason, and P. Pauling, *Inorg. Chem.*, **4**, 456 (1965).

(3) M. A. Porai-Koshits, *Russ. J. Inorg. Chem.*, **1**, 332 (1959).

(4) L. E. Orgel, Report to the Xth Solvay Council, Brussels, 1956, pp 289–338.

(5) H. A. Jahn and E. Teller, *Proc. Roy. Soc.* (London), **A161**, 220 (1937).